Anticancer activity of Ru- and Os(arene) compounds of a maleimide-functionalized bioactive pyridinecarbothioamide ligand

Muhammad Hanif,[a] Sally Moon,[a] Matthew P. Sullivan,[a,b] Sanam Movassaghi,[a] Mario Kubanik,[a] David C. Goldstone,[b] Tilo Söhnel,[a] Stephen M. F. Jamieson,[c] and Christian G. Hartinger[a,*]

[a] *School of Chemical Sciences, University of Auckland, Private Bag 92019, Auckland 1142, New Zealand.*
[b] *School of Biological Sciences, University of Auckland, Private Bag 92019, Auckland 1142, New Zealand.*
[c] *Auckland Cancer Society Research Centre, University of Auckland, Private Bag 92019, Auckland 1142, New Zealand.*

* School of Chemical Sciences, University of Auckland, Private Bag 92019, Auckland 1142, New Zealand.
E-mail: c.hartinger@auckland.ac.nz; Fax: (+64)9 373 7599 ext 87422

Keywords:

Ru(arene) complexes; anticancer agents; bioorganometallics; albumin carrier; maleimide

Abstract

With the aim of increasing the accumulation of Ru anticancer agents in the tumor, a targeted delivery strategy based on a maleimide anchor for the biological vector human serum albumin (HSA) was developed. A group of piano stool Ru and Os(η^6-arene) complexes carrying a maleimide-functionalized *N*-phenyl-2-pyridinecarbothioamide (PCA) ligand was designed allowing for covalent conjugation to biological thiols. The complexes were characterized by NMR spectroscopy, ESI-MS, elemental analysis and single-crystal X-ray diffraction analysis. The compounds were shown to undergo halido/aqua ligand exchange reactions in aqueous solution, depending mainly on the metal center and the nature of the halide. *In vitro* cytotoxicity studies revealed low potency which is explained by the observed high reactivity of the maleimide to the thiol of L-cysteine (Cys), while the metal center itself shows little affinity to amino acids of the model protein lysozyme.

Introduction

Since the approval of cisplatin for clinical use in 1978 [1], many metal complexes have been assayed on their tumor-inhibiting properties. Based on similar ligand exchange kinetics, ruthenium(III) was identified early as a viable alternative to platinum in anticancer drug development. Many examples of ruthenium complexes are being studied preclinically, with a small number of coordination compounds having progressed into clinical testing, including imidazolium *trans*-[tetrachlorido(dimethylsulfoxide)(1*H*-imidazole)ruthenate(III)] NAMI-A, which recently failed at phase II, and sodium *trans*-[tetrachloridobis(1*H*-indazole)ruthenate(III)] (NKP-1339/IT139), derived from the earlier studied KP1019, being currently undergoing clinical studies [2]. Over the last 20 years nearly all transition metals have been considered in anticancer drug development. With the emergence of the anticancer activity of organometallic titanocene dichloride, also organoruthenium and later organoosmium compounds were introduced [3-5]. Promising compounds currently under preclinical development include [dichlorido(η^6-*p*-cymene)(1,3,5-triaza-7-phosphatricyclo[3.3.1.1]decane)ruthenium(II)] (RAPTA-C) and [chlorido(η^6-*p*-cymene)(1,2-diaminoethane)ruthenium(II)] hexafluorophosphate (RAED-C) [6]. RAPTA-C features a 1,3,5-triaza-7-phosphaadamantane (PTA) and two chlorido ligands coordinated to the Ru(η^6-*p*-cymene) [Ru(cym)] fragment. It shows promising effects on solid tumor metastases while RAED-C equipped with a bidentate ethylenediamine and a chlorido co-ligand at the Ru(cym) moiety reduces the growth of primary tumors [7]. Furthermore, when RAPTA-C was used in a combination regime, it efficiently inhibited tumor growth while exhibiting no side effects [8,9]. The differences in the modes of action observed for these organoruthenium compounds were highlighted by the distinctive chemical properties. It was shown that the preferential binding site of these molecules to the nucleosome core, featuring both DNA and proteins, was different. While RAED-C was found attached to DNA, RAPTA-C was found bound to the proteinaceous histone core [10]. This shows the importance of the ligands coordinated to the metal centers. However, besides showing potential as anticancer chemotherapeutics [3,4,11], these small-molecule scaffolds lack the selectivity required to target the tumor or tumor cells over healthy tissue.

Many strategies have been suggested to improve drug accumulation in tumor tissue. These involve the use of macromolecular carrier systems, such as nanoparticles, micelles and proteins, all of which have been established to be efficacious in delivering pharmacophores [12-19]. Macromolecules and nanoparticles can extravasate into tumor tissue *via* leaky vessels exploiting the enhanced permeability and retention (EPR) effect, which is related to an increased permeability of macromolecules from the blood vessels into tumors [20-23]. In particular the transport mediated by serum proteins has attracted a lot of attention in the development of metal-based drugs. It has been suggested that Ru^{III} complexes may be carried by transferrin due to the similarity to Fe^{III}. More recently, we have however shown that the majority of drug for the clinical candidates KP1019 and NKP-1339/IT139 is attached *in vivo* to albumin [24,25]. In the 1990s, cisplatin was reacted with human serum albumin (HSA) and transferrin and in contrast to common belief of deactivation, the drug conjugates still showed anticancer activity in clinical trials [26,27]. Loading HSA covalently with metallodrugs led recently to an improvement of the tumor-inhibiting properties of a non-cytotoxic Ru(II) compound by a significant degree [28]. Kratz *et al.* were successful in designing maleimide-functionalized linkers for Pt complexes (Figure 1, top) which reacted with HSA after intravenous administration [29]. Maleimides are known to react selectively with cysteine residues, such as Cys34 in HSA [30]. This HSA conjugation strategy has proven efficacious also for organic drugs with the approval of albumin-bound doxorubicin for use in the treatment of breast cancer (Figure 1, bottom) [14,31,32]. We recently reported the first ruthenium-compound, Mal-RAPTA, to exploit the EPR effect by functionalizing RAPTA-C with a maleimide moiety [33]. In that case we introduced the maleimide functional group at the arene, as its variation was shown to have less impact on the biological activity than functionalizing the PTA ligand [34,35]. More recently, we reported Ru(arene) complexes of indazole and pyridine functionalized with maleimide [36]. The reactivity of the compounds to biological thiols was similar to Mal-RAPTA and they exhibited potent anticancer activity.

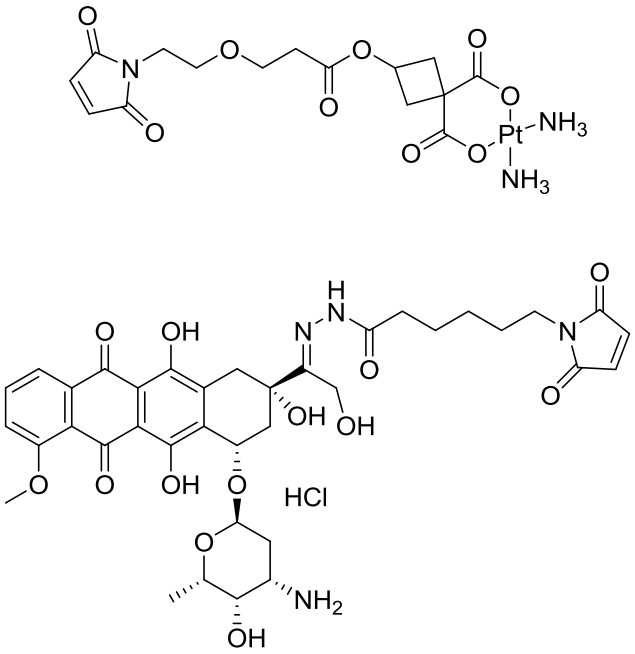

Figure 1. Anticancer agents exploiting the maleimide-based albumin conjugation strategy.

Here we report the development of *N*-maleimide substituted 2-pyridinecarbothioamide (PCA) complexes. We observed for the non-maleimide functionalized analogs such as [chlorido(η^6-*p*-cymene)(*N*-{4-fluorophenyl}-2-pyridinecarbothioamide)ruthenium(II)] chloride (Ru-PCA) that they were potent in inhibiting cancer cell growth [37]. The stability of these complexes even under acidic conditions suggests their potential as orally administrable anticancer agents. By introducing a maleimide group at the PCA ligand, we aimed for compounds of similar potency but with potential to exploit the targeting properties of HSA after reaction in the bloodstream to exploit the EPR effect.

Results and discussion

After establishing that a maleimide at the arene ring resulted in *in vitro* anticancer activity similar to the parent compound [33], the aim of this study was to elucidate the impact of introducing a maleimide moiety into the ancillary ligand of anticancer active Ru-PCA complexes [37].

The introduction of the maleimide group into a PCA ligand was carried out in two steps to obtain *N*-(4-(maleimidyl)phenyl)pyridine-2-carbothioamide **1** (Scheme 1). Firstly, a solution of *N*-(4-aminophenyl)pyridine-2-thiocarboxamide in dry dichloromethane was added dropwise to a solution of maleic anhydride at a molar ratio of 1 : 1, which resulted in the immediate formation of a yellow precipitate. It was further stirred for 1 hour to ensure completion of the reaction. Then the suspension was filtered to afford the ring-open maleic amide intermediate (*Z*)-4-oxo-4-[(4-(pyridine-2-carbothioamido)-phenyl)amino]but-2-enoic acid. The maleic amide intermediate was characterized by ^{1}H NMR spectroscopy in DMSO-d_6. The peak pattern and their multiplicities were similar to those observed for the precursor *N*-(4-aminophenyl)pyridine-2-thiocarboxamide. In addition, signals indicating the formation of the maleic amide intermediate were identified. The CONH functionality gave a signal at 10.51 ppm while the carboxylic acid proton was detected downfield at 13.10 ppm. The two protons from the maleic acid gave doublets at 6.50 and 6.32 ppm.

To obtain maleimide **1**, a mixture of the ring-open maleic amide intermediate and sodium acetate in acetic anhydride was stirred at 95 °C for 30 minutes. The dark brown solution was poured in ice water, resulting in precipitation of a yellow solid, which was filtered off and washed with water. Alternatively, the product was obtained by extraction from water and dichloromethane (DCM). The solvent was evaporated to gain **1** as a yellow solid which was further purified by filtration of a DCM solution through a plug of silica gel. Pure *N*-(4-(maleimidyl)phenyl)pyridine-2-carbothioamide **1** was obtained as a bright orange solid with a yield of 75%.

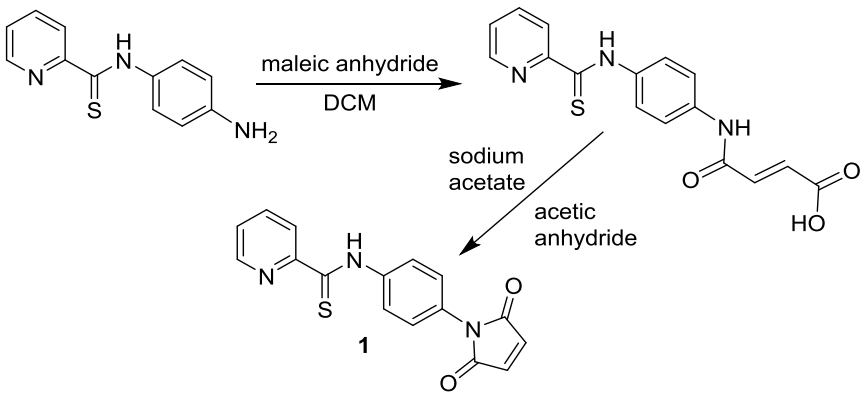

Scheme 1. Synthesis of *N*-(4-(maleimidyl)phenyl)pyridine-2-carbothioamide **1**.

N-(4-(Maleimidyl)phenyl)pyridine-2-carbothioamide **1** was characterized by ^{1}H and ^{13}C{^{1}H} NMR spectroscopy, electrospray ionization mass spectrometry (ESI-MS) and elemental analysis. The chemical shifts of the proton signals in the ^{1}H NMR spectrum changed slightly as compared to that of the *N*-(4-aminophenyl)pyridine-2-thiocarboxamide precursor, *i.e.*, the CSNH proton was shifted downfield by 0.26 ppm, as were H9/H10 (Δδ = 0.42 ppm) and H11/H12 (Δδ = 0.74 ppm). This may be explained by the introduction of the maleimide moiety and the electronegativity of the two carbonyl groups causing deshielding of these protons. The formation of the maleimide moiety was clearly confirmed as the two separate doublets assigned to the maleic CH protons in the ring-opened intermediate were absent in the spectrum and a singlet at 6.87 ppm was detected and assigned to the maleimide CH protons. The formation of the maleimide was also shown by ESI-MS. The base peak was detected at *m/z* 332.0474 which matches well to the theoretical *m/z* value for the sodium adduct $[M + Na]^{+}$ (m/z_{calc} 332.0464).

Compound **1** was converted with a variety of $[M(\eta^6\text{-arene})X_2]_2$ dimeric precursors (M = Ru, Os; arene = *p*-cymene, biphenyl; X = Cl, Br, I) into the respective $[M(\eta^6\text{-arene})(\mathbf{1})X]X$ complexes. To obtain these compounds, **1** was added to the $[M(\eta^6\text{-arene})X_2]_2$ dimer in absolute dichloromethane. In case of the $[M(\eta^6\text{-biphenyl})Cl_2]_2$ dimers, 2–3 mL of dimethylformamide was added to assist dissolution of the dimer. After allowing the reaction to proceed for 4 h at room temperature, the solvent was evaporated and the residue was dissolved in a minimal volume of DCM. Dropwise addition to cold diethyl ether resulted in immediate precipitation of the product and the mixture was kept in the fridge overnight. The formed precipitate was filtered,

washed with cold diethyl ether and dried under vacuum to afford the desired complexes **2a–g** in 38–91% yield.

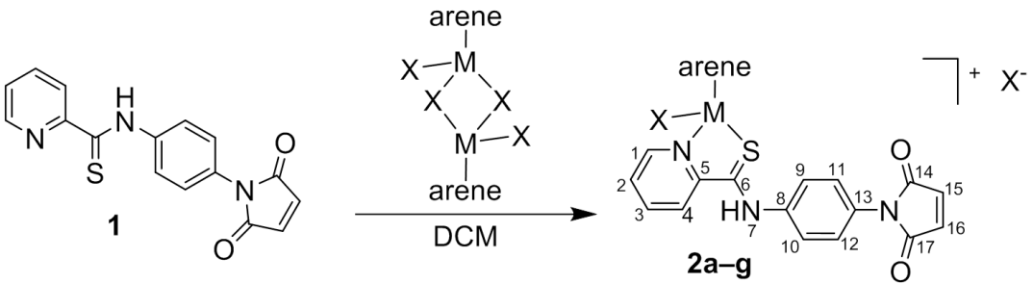

arene =

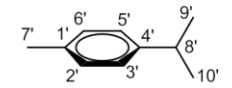

***p*-cymene**

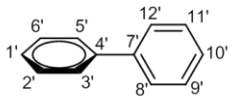

biphenyl

compound	arene	M	X
2a	*p*-cymene	Ru	Cl
2b	*p*-cymene	Ru	Br
2c	*p*-cymene	Ru	I
2d	*p*-cymene	Os	Cl
2e	*p*-cymene	Os	I
2f	biphenyl	Ru	Cl
2g	biphenyl	Os	Cl

Scheme 2. Synthesis of [M(η^6-arene)] complexes **2a**–**g** from *N*-(4-(maleimidyl)phenyl)pyridine-2-carbothioamide **1** with the NMR numbering scheme.

The chemical shifts observed in the ^{1}H and ^{13}C{^{1}H} NMR spectra of the complexes **2a**–**e** are similar to those observed from uncoordinated **1** and the [MX_2(η^6-*p*-cymene)]$_2$ dimer. Due to the coordination of the ligand to the metal center, both the peaks from the PCA-maleimide ligand and the cymene are slightly shifted. In order to unambiguously assign peaks at the thiocarbamide ligand and the cymene, the complexes were further analyzed by 2D NMR techniques, such as ^{1}H-^{1}H COSY, ^{1}H-^{13}C{^{1}H} HSQC and ^{1}H-^{13}C{^{1}H} HMBC NMR spectroscopy. In the ^{1}H NMR spectra, the maleimide CH protons (H_{15}/H_{16}) appeared as sharp singlets at around 7.0 ppm for **2a**–**g**. H_{11} and H_{12} at 8.0 ppm couples with H_9 and H_{10} at 7.5 ppm. Likewise, H_2 at 7.60 ppm couples with H_3 at 8.16 ppm, whereas the adjacent proton H_1 at 9.3 ppm also displayed coupling with H_2. Similarly proton-proton coupling was seen for the arene fragment with the $H_{8'}$ at 2.8 ppm coupling with $H_{9'}$ and $H_{10'}$ at 1.3 and 1.2 ppm. The four aromatic protons $H_{2'}$, $H_{3'}$, $H_{5'}$ and $H_{6'}$ couple to each other at 5.7–5.4 ppm. In the ^{13}C{^{1}H} NMR spectra, the $C_{1'}$ and $C_{4'}$ were identified at 103.0 and 106.3 ppm

respectively, while the *C*H of the arene ligands were present in the range of 84–91 ppm for Ru complexes **2a**–**c** and **2f** as well as 76–82 ppm for the Os complexes **2d**, **2e** and **2g**. The signals assigned to C_6 were only detectable for **2c** and **2f** at around 191 ppm. C_{14} and C_{17} were assigned to signals at *ca.* 170 ppm due to the strong coupling with H_{15} and H_{16}, as shown in the HMBC spectra. The maleimide *C*H signals were found at approximately 135 ppm as a single peak due to symmetry, as was also observed in the ^{1}H NMR spectra.

The identity of complexes **2a–g** was further confirmed by ESI-MS. The compounds were detected as their $[M - 2X - H]^+$ ions in positive ion modes. The experimental *m/z* values were in good agreement with the calculated values of each complex.

The molecular structure of complex **2b** was resolved by single-crystal X-ray diffraction analysis. The crystals were obtained by slow diffusion of diethyl ether into a solution of **2b** in dichloromethane. Compound **2b** crystalized in the *C*2/*c* monoclinic space group.

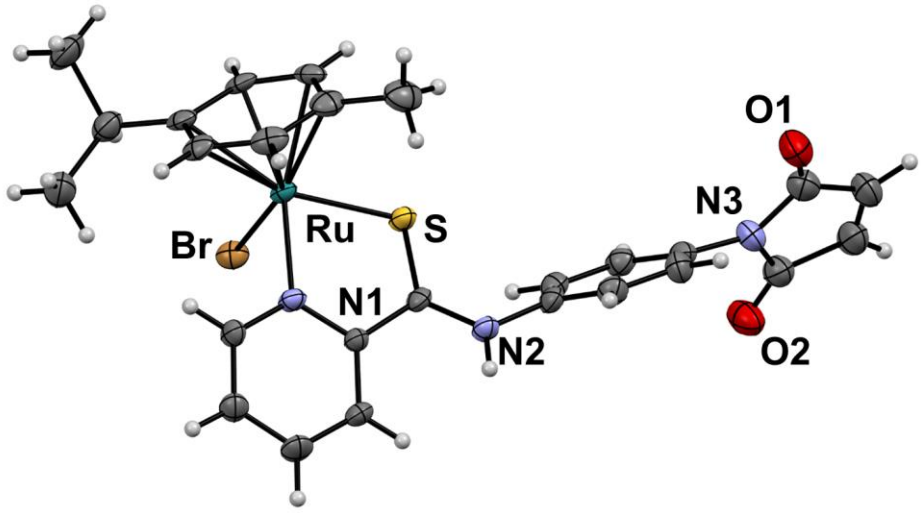

Figure 2. The molecular structure of **2b** drawn at 50% probability with the heteroatoms labelled. The counter anion and solvent molecules were removed for clarity.

The overall structure of the complex was very similar to that of the reported thiocarbamide complex [37]. The complex features the common piano-stool geometry where the metal center is coordinated to the η^6-*p*-cymene ring, an *S*,*N*-chelating *N*-(4-(maleimidyl)phenyl)pyridine-2-carbothioamide ligand, and a bromido ligand. The overall +1 charge of the complex was counter-balanced by a bromide in the second coordination sphere (Figure 2).

The distance between the metal center and the η^6-*p*-cymene centroid was 1.697(4) Å, which is in similar range as observed for a structurally-related Ru-PCA complex [37]. When comparing the Ru–X distance in Ru-PCA (X = Cl) and the Ru–Br bond length in **2b**, the latter was, as expected, significantly longer at 2.5355(7) *vs* 2.3924(4) Å. The Ru–S and Ru–N(1) bond lengths were 2.3392(14) and 2.111(4) Å, respectively, and were virtually uninfluenced by the substitution of the phenyl ring with the maleimide moiety (2.341 and 2.095 Å in Ru-PCA) [37]. Replacing the chlorido ligand in Ru-PCA with a bromido in **2b**, the S–Ru–Br, N(1)–Ru–Br and S–Ru–N(1) angles were only slightly impacted and angles of 88.59°, 84.61° and 81.70°, respectively, were observed. The phenyl ring was twisted out of plane by 54.7° and the maleimide ring was further twisted from the phenyl ring at 46.95°.

Table 1. Selected bond lengths (Å), angles (°) and torsion angles (°) of **2b** as compared to Ru-PCA [37].

Bond Lengths (Å)	**2b** (X = Br)	**Ru-PCA** (X = Cl)
Ru–S	2.3392(14)	2.3414(9)
Ru–N1	2.111(4)	2.095(3)
Ru–X	2.5355(7)	2.3924(4)
Ru–centroid	1.697(4)	1.687(3)
Bond Angles (°)		
S–Ru–N1	81.70(13)	81.28(8)
S–Ru–X	88.59(4)	89.81(3)
N1–Ru–X	84.61(13)	83.68(8)
Torsion Angles (°)		
C6–N2–C7–C8	53.92(11)	52.7(5)
N1–C5–C6–S	15.62(10)	15.9(4)

Many potent anticancer agents suffer from limited aqueous solubility and stability. This is also true for organometallic complexes, especially when bearing extended ligand systems. This is the reason why especially for biological and bioanalytical studies, stock solutions in DMSO are employed. We have demonstrated that bidentate *S*,*N*-chelating ligands led to highly stable organoruthenium and -osmium compounds due to their strong bonding to the metal(II) center [37]. In fact, these compounds were even resistant to acidic conditions which led to the suggestion of

their applicability as oral anticancer agents. However, the halogenido co-ligand may undergo ligand exchange reactions to form bioactive adducts with essential biomolecules. In order to confirm these observations for the newly synthesized complexes, **2a**, **2d** and **2f** were selected for stability studies by means of ^{1}H NMR spectroscopy. The ^{1}H NMR spectra were measured in 5% aqueous DMSO solution at room temperature. The Ru(II) complex **2a** showed an estimated half-life of less than 3 h, and after 72 h about 95% of the compound had undergone a ligand exchange reaction in aqueous solution (Figure 3).

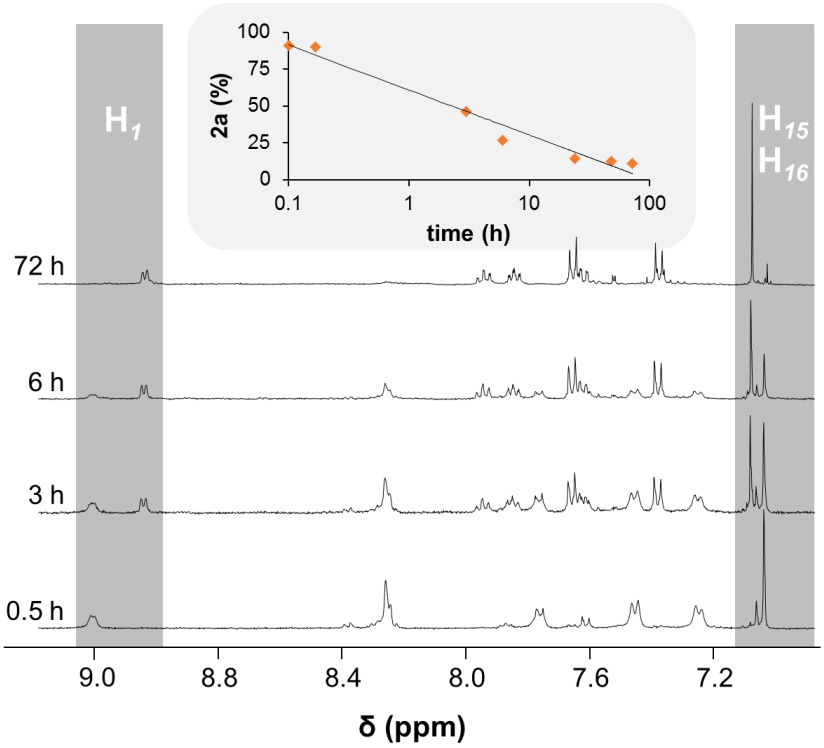

Figure 3. Aqueous stability of **2a** in 5% DMSO-d_6/D_2O studied by ^{1}H NMR spectroscopy.

In contrast to the Ru complex, the analogous Os(II) derivative **2d** was significantly more stable with the half-life not reached even after 96 hours of incubation (Figure S1). The hydrolytic stability of Os complexes is often higher than of the Ru congeners due to the lower ligand exchange reaction rates. For example, $Os^{II}(\eta^{6}$-*p*-cymene)(ethylenediamine)Cl undergoes a chlorido/aqua exchange reaction approximately 40-times slower than its Ru(II) analogue [37]. The chlorido and bromido complexes showed comparable results in terms of ligand exchange reactions while the iodido/aqua exchange was considerably suppressed.

When comparing the stability of the [Ru(η^6-*p*-cymene)Cl] and [Ru(η^6-biphenyl)Cl] complexes **2a** and **2f** at room temperature, for **2a** about 10% of the complex was found aquated immediately upon dissolution in 5%DMSO-d_6/D_2O and more than 50% within three hours. After 72 hours, only 11% of unhydrolyzed species was detectable. A similar behavior was observed for **2f** and it appears that for both complexes an equilibrium between the different species in the reaction mixture was formed.

The [M(η^6-arene)] complexes **2a**, **2b** and **2e** as representative examples were subjected to anticancer activity studies against human colorectal carcinoma (HCT116) and human breast adenocarcinoma (MDA-MB-231) cell lines. Surprisingly, none of the complexes showed significant growth inhibition of cancer cell lines (IC_{50} values > 400 µM or IC_{50} not reached at the highest used concentration), as compared to the non-maleimide bearing Ru-PCA and related complexes [37]. Therefore, the other compounds were not tested on their biological activity.

In order to explain the low potency against tumor cells, bioanalytical studies were conducted. Electrospray ionization mass spectrometry (ESI-MS) and protein X-ray crystallography were used to elucidate the interaction between **2a** and hen egg white lysozyme (HEWL) which is devoid of free thiol groups. The ESI-MS studies showed that after a period of five days no interaction had occurred (Supporting Information). X-ray crystallographic experiments indicated that there was a ruthenium-containing molecule held in the crystal lattice but it was detected in the space between two symmetry units. There was, however, significant electron density that surrounded the modelled ruthenium center. Attempts to model the structure of **2a** into the areas of residual electron density proved to be challenging, most likely due to a mixed population of low occupancy states (Supporting Information). These experiments show that the reactivity of the Ru center to proteins is limited. However, the design hypothesis behind the development of maleimide-functionalized cytotoxins is that they may react *in vivo* with HSA and exploit thereby HSA as a vector to the tumor site. HSA features a single thiol group in form of cysteine-34 which should allow efficient and selective conjugation of the cytotoxin to the protein.

Given this notion, the thiol-binding ability of [MX(η^6-arene)] complexes was investigated by means of ^{1}H NMR spectroscopy. The complexes were dissolved in 5% DMSO-d_6/D_2O and a solution of L-cysteine (Cys) was added in small portions

(1.2 equivalents). The ^{1}H NMR spectra were recorded until the signal assigned to the maleimide protons H_{15} and H_{16} at approximately 7.0 ppm disappeared. The DMSO peak was used as an internal standard while following the reaction. As observed for other maleimide-functionalized compounds [33,36], complexes **2a**, **2b**, **2d** and **2f** reacted very quickly with Cys and the reaction was completed within about 40 mins (Figure 4 for **2d**).

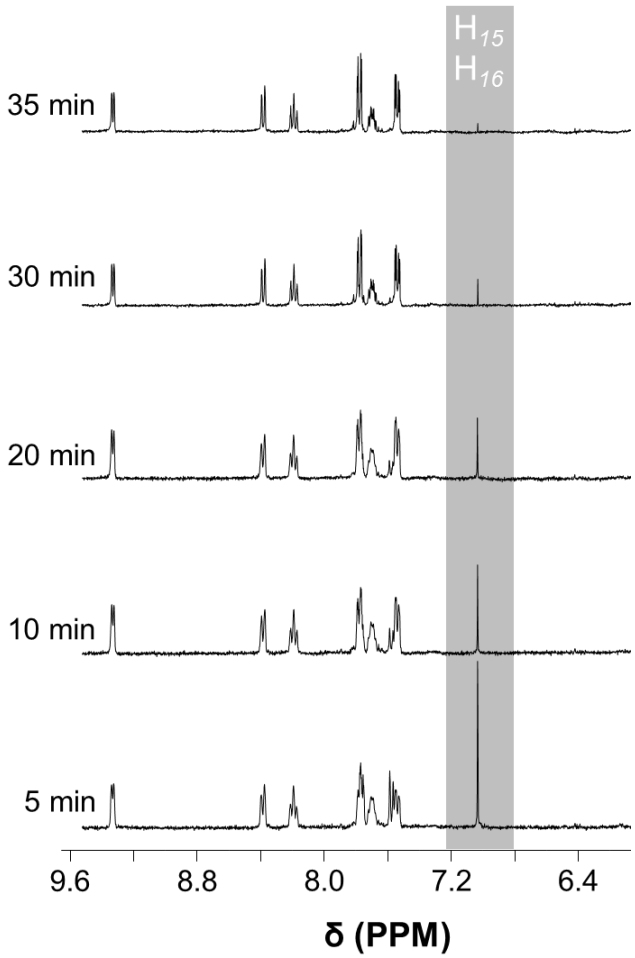

Figure 4. Time-dependent reaction of the Os complex **2d** with L-cysteine in 5% DMSO-d_6/D_2O.

This shows that the compounds react very selectively through the maleimide residue with biomolecules while the Ru center does not form covalent bonds with proteins. In contrast, ^{1}H NMR spectroscopy of mixtures of **2a** and L-histidine or L-methionine showed adduct formation through coordination at the metal center while only minor amino acid adducts could be detected by ESI-MS. The high reactivity of the Ru complexes towards Cys may however be the reason for the low biological activity.

Cell media are supplemented with proteins such as albumin from fetal calf serum which may interfere with the biological activity, as the proteins react quickly with the maleimide group. The PCA ligand plays an important role in the cytotoxicity of organoruthenium and -osmium compounds [37] and anchoring it to a protein may result in deactivation, as compared to functionalizing the arene ligand which did not impact the cytotoxic activity of Ru(arene) complexes [33].

Conclusions

Ru- and Os(η^6-arene) complexes have been extensively researched as antitumor agents. These complexes have been fine-tuned by careful design and selection of arenes and biologically active ligands. However, as most small molecule anticancer agents, they often lack tumor selectivity which may result in side effects during treatment. Biological macromolecular vectors, such as HSA, are an ideal platform to enhance the accumulation of cytotoxins in the tumor through the EPR effect. Such a delivery strategy maximizes the antiproliferative activity of the drug, while reducing the systemic toxicity to non-tumorigenic tissue.

Therefore, we present here a strategy to introduce a maleimide moiety into the ligand framework of cytotoxic Ru complexes bearing a PCA ligand. We have shown before that maleimide-functionalized Ru complexes react selectively through their maleimide residue with Cys, while the Ru center is not involved in the interaction [33], and this allows selective modification of Cys-34 of HSA. Employing the same strategy resulted in the successful introduction of a maleimide residue on the PCA *N*-(4-aminophenyl)pyridine-2-thiocarboxamide. This ligand was used to prepare organometallic Ru and Os complexes with varying arene and leaving halido ligands. The molecular structure of the [Ru(η^6-*p*-cymene)Br] derivative **2b** was determined by X-ray diffraction analysis.

The complexes were shown to undergo a ligand exchange reaction involving the halido ligand at the metal center while the bidentate *S*,*N*-chelating ligand remained coordinated. As expected, the hydrolysis rate of the Ru complex was faster than that of its Os congener. When chlorido and bromido ligands were present as the leaving groups, comparable results were obtained, whereas the hydrolysis of iodido derivatives was notably suppressed. Representative complexes were subjected to *in*

vitro anticancer activity studies in the human cancer cell lines HCT116 and MDA-MB-231. Surprisingly very low anticancer activity was observed, given that the PCA complexes are low μM cell growth inhibitors. To explain this observation, their reactivity to a model protein containing no free thiol group and L-cysteine was investigated. The compounds did not react with the protein, as demonstrated by ESI-MS, however, in an X-ray crystallographic study residual electron density was detected but no coordination of the Ru center to amino acids could be observed. When examining the reactivity of the complexes with L-cysteine by means of ^{1}H NMR spectroscopy, complete conjugation of the thiol group was observed in a timeframe of about 40 min, largely independent of the metal center, leaving group and arene. The fact that the bioactive moiety, *i.e.*, the PCA ligand, was functionalized with the maleimide and therefore eventually is anchored on the HSA carrier is suggested as the reason for the low potency of this complex type in biological assays, as the bioactive moiety remains covalently bound to albumin from the growth medium for the cancer cells.

Acknowledgements

We thank the University of Auckland, the Austrian Science Fund (Schrödinger fellowship to M.H.), the India-New Zealand Education Council, Education New Zealand, the India-New Zealand Research Institute, the Royal Society of New Zealand and COST CM1105 for funding. This research was, in part, undertaken on the microcrystallography beamline (MX2) at the Australian Synchrotron, Victoria, Australia. D.G. is supported by a Rutherford Discovery Fellowship awarded by the NZ government and administered by the RSNZ. We thank the National Institutes of Health and National Cancer Institute for grant 1R13CA200223-01A1 (Conference Organization support, 1st International Symposium on Clinical and Experimental Metallodrugs in Medicine: Cancer Chemotherapy, CEMM).

Experimental

Materials and methods

All air-sensitive reactions were carried out under nitrogen in standard Schlenk flasks. Reactions involving Ru(II) and Os(II) precursors were protected from light by using aluminum foil. Dichloromethane (DCM), diethyl ether (Et_2O), acetonitrile (ACN), chloroform and tetrahydrofuran (THF) were dried through a solvent purification system (LC Technology Solutions Inc., SP-1 solvent purifier) and transferred into Schlenk flasks that were dried under high vacuum and degassed with N_2 prior to use. Ethanol (EtOH) and methanol (MeOH) were dried over activated molecular sieves (3Å) in a N_2 Erlenmeyer flask for two days prior to use. Thin layer chromatography (TLC) was performed on aluminum sheets pre-coated with Merck silica gel 60 F254. 1,4-Phenylenediamine (Sigma-Aldrich, ≥99.5%), 2-methylpyridine (Sigma-Aldrich, 98%), acetic anhydride (ECP, 99%), α-terpinene (Sigma-Aldrich, 89%), biphenyl (Sigma-Aldrich, 99.5%), L-histidine (AK Scientific, 98%), L-methionine (AK Scientific, 98%), ethanol (ECP, AR grade), maleic anhydride (Sigma-Aldrich, 99%), anhydrous *N*,*N*-dimethylformamide (Sigma-Aldrich, 99.8%), osmium tetroxide (Johnson Matthey Materials Technology UK, 98%), potassium bromide (Sigma-Aldrich, ≥99.0%), potassium iodide (Sigma-Aldrich, AR), $RuCl_3 \cdot 3H_2O$ (PMO, 99%), sodium acetate (ECP, 99%), sodium sulfide nonahydrate (Sigma-Aldrich, ≥98.0%) and sulfur (Sigma-Aldrich) were purchased from commercial suppliers and used as such. The dimers bis[dichlorido(η^6-*p*-cymene)ruthenium(II)] [38], bis[dibromido(η^6-*p*-cymene)ruthenium(II)], bis[diiodido(η^6-*p*-cymene)ruthenium(II)] [39], bis[dichlorido(η^6-*p*-cymene)osmium(II)], bis[diiodido(η^6-*p*-cymene)osmium(II)] [40,41], bis[dichlorido(η^6-biphenyl)ruthenium(II)] [39] and the *N*-(4-aminophenyl)pyridine-2-thiocarboxamide [42] were synthesized by adapting reported procedures.

1D and 2D NMR spectra were recorded on Bruker DRX 400 MHz NMR spectrometers at ambient temperature. The measurement frequency for ^1H and $^{13}C\{^1H\}$ NMR spectra was 400.13 and 100.61 MHz. Melting points were measured on a Bibby Stuart Scientific Melting Point Apparatus SMP3 using capillary tubes. Elemental analysis was performed at the Campbell Microanalytical Laboratory, The University of Otago. ESI-mass spectra data were recorded on a Bruker micrOTOF-Q II mass spectrometer in positive ion electrospray ionization (ESI) mode.

The X-ray diffraction data of **2b** (CCDC 1471034) was collected on a Bruker Smart APEX II diffractometer with graphite-monochromatized Mo*Kα* radiation, λ_{Mo} = 0.71073 Å at 100 K (see Supporting Information for the measurement parameters). Data reduction was carried out using the SAINT program [43]. Semi-empirical absorption corrections were applied based on equivalent reflections using SADABS [44]. The structure solution and refinements were performed with the SHELXS-97 and SHELXL-2013 program packages [45].

Syntheses

N-(4-(Maleimidyl)phenyl)pyridine-2-carbothioamide, ***1***

Maleic anhydride (0.98 g, 10.0 mmol) in anhydrous dichloromethane (DCM, 20 mL) was added dropwise to a solution of *N*-(4-aminophenyl)pyridine-2-thiocarboxamide (2.29 g, 10.0 mmol) in anhydrous DCM (30 mL). The mixture immediately turned into an orange/yellow solution and a yellow precipitate formed. It was stirred for 2 h at room temperature under N_2. Then the solvent was evaporated to afford (*Z*)-4-oxo-4-[(4-(pyridine-2-carbothioamido)phenyl)amino]but-2-enoic acid as a light orange/yellow powder. This intermediate was used for the next step without further purification.

Yield: 3.22 g (98%); ^{1}H NMR (DMSO-d_6, 400.13 MHz): δ (ppm) = 13.10 (brs, 1H, CO*OH*), 12.26 (s, 1H, CS*NH*), 10.51 (s, 1H, CO*NH*), 8.68 (ddd, $^3J_{(H3, H4)}$ = 5 Hz, $^4J_{(H2, H4)}$ = 2 Hz, $^5J_{(H1, H4)}$ = 1 Hz, 1H, H_4), 8.54 (ddd, $^3J_{(H1, H2)}$ = 5 Hz, $^4J_{(H1, H3)}$ = 2 Hz, $^5J_{(H1, H4)}$ = 1 Hz, 1H, H_1), 8.05 (dt, $^3J_{(H2, H3)/(H3, H4)}$ = 8 Hz, $^4J_{(H1, H3)}$ = 2 Hz, 1H, H_3), 7.98 (d, $^3J_{(H9, H11)/(H10, H12)}$ = 9 Hz, 2H, H_{11}, H_{12}), 7.70 (d, $^3J_{(H9, H11)/(H10, H12)}$ = 9 Hz, 2H, H_9, H_{10}), 7.66 (ddd, $^3J_{(H2, H3)}$ = 8 Hz, $^3J_{(H1, H2)}$ = 5 Hz, $^4J_{(H2, H4)}$ = 2 Hz, 1H, H_2), 6.50 (d, $^3J_{(H15, H16)}$ = 12 Hz, 1H, H_{15}), 6.32 (d, $^3J_{(H15, H16)}$ = 12 Hz, 1H, H_{16}).

(*Z*)-4-oxo-4-[(4-(pyridine-2-carbothioamido)phenyl)amino]but-2-enoic acid (0.33 g, 1.0 mmol) and sodium acetate (0.04 g, 0.5 mmol) were dispersed in acetic anhydride (15 mL) and the mixture was heated to ~90 °C for 30 minutes. The resulting dark brown solution was cooled to room temperature, and it was added dropwise to ice water to form a brown precipitate. It was filtered, washed thoroughly with water and dried. The purification was achieved by dissolving the crude product in DCM and filtration through a plug of silica. The collected filtrate was evaporated to afford pure *N*-(4-(maleimidyl)phenyl)pyridine-2-carbothioamide as a bright orange solid.

Yield: 0.24 g (75%); m. p.: 193–196 C; ^{1}H NMR ($CDCl_3$, 400.13 MHz): δ (ppm) = 12.15 (brs,1H, CS*NH*), 8.79 (dd, $^{3}J_{(H3, H4)}$ = 8 Hz, $^{4}J_{(H2, H4)}$ = 1 Hz, 1H, H_4), 8.56 (ddd, $^{3}J_{(H1, H2)}$ = 5 Hz, $^{4}J_{(H1, H3)}$ = 2 Hz, $^{5}J_{(H1, H4)}$ = 1 Hz, 1H, H_1), 8.25 (d, $^{3}J_{(H9, H11)/(H10, H12)}$ = 9 Hz, 2H, H_{11}, H_{12}), 7.90 (dt, $^{3}J_{(H2, H3)/(H3, H4)}$ = 8 Hz, $^{4}J_{(H1, H3)}$ = 2 Hz, 1H, H_3), 7.48 (ddd, $^{3}J_{(H2, H3)}$ = 8 Hz, $^{3}J_{(H1, H2)}$ = 5 Hz, $^{4}J_{(H2, H4)}$ = 1 Hz, 1H, H_2), 7.47 (d, $^{3}J_{(H9, H11)/(H10, H12)}$ = 9 Hz, 2H, H_9, H_{10}), 6.87 (s, 2H, H_{15}, H_{16}); ^{13}C{^{1}H NMR ($CDCl_3$, 100.6 MHz): δ (ppm) = 188.0 (C_6), 169.3 ($C_{14,}$ C_{17}), 151.4 (C_5), 146.6 (C_1), 138.1 (C_{13}), 137.6 (C_3), 134.3 ($C_{15,}$ C_{16}), 128.9 (C_8), 126.3 (C_9, C_{10}), 126.2 (C_2), 124.8 (C_4), 123.0 (C_{11}, C_{12}); MS (ESI$^+$): *m/z* 332.0464 $[M + Na]^+$ (m_{ex} = 332.0474); elemental analysis calculated for $C_{16}H_{11}N_3O_2S{\cdot}0.5H_2O$: C 60.36, H 3.80, N 13.20%. Found: C 60.60, H 3.61, N 13.24%.

General procedure for the synthesis of [M(η^6-arene)] complexes of N-(4-(maleimidyl)phenyl)pyridine-2-carbothioamide ***2a–g***

$[M(\eta^6\text{-arene})]_2$ dimer (1 equiv.) was dissolved in absolute DCM (20 mL). In the case of $[M(\eta^6\text{-biphenyl})Cl_2]_2$ dimers, 2–3 mL of dimethylformamide (DMF) was added to assist the full dissolution of the dimer. *N*-(4-(Maleimidyl)phenyl)pyridine-2-carbothioamide (2 equiv.) was added to the solution of the dimer and the reaction mixture was stirred for 4 h at room temperature. The solvent was evaporated, and the residue was dissolved in a minimal volume of DCM. This solution was added dropwise to cold diethyl ether, which resulted in immediate precipitation of the product. After placing it in the fridge overnight, the precipitate was filtered, washed with cold diethyl ether and dried under high vacuum to afford the desired complexes.

Chlorido[N-(4-(maleimidyl)phenyl)pyridine-2-carbothioamide](η^6-p-cymene)ruthenium(II) chloride, ***2a***

The synthesis was performed according to the general procedure using *N*-(4-(maleimidyl)phenyl)pyridine-2-carbothioamide (111 mg, 0.36 mmol) and $[Ru(\eta^6\text{-}p\text{-cymene})Cl_2]_2$ (110 mg, 0.18 mmol) to afford **2a** as an orange solid.

Yield: 191 mg (83%); m. p.: 171–174 °C (decomp.); ^{1}H NMR ($CDCl_3$, 400.13 MHz): δ (ppm) = 9.44 (brs, 1H, H_4), 9.39 (d, $^{3}J_{(H1, H2)}$ = 6 Hz, 1H, H_1), 8.09 (t, $^{3}J_{(H2, H3)/(H3, H4)}$ = 8 Hz, 1H, H_3), 7.93 (d, $^{3}J_{(H9, H11)/(H10, H12)}$ = 8 Hz, 2H, H_{11}, H_{12}), 7.58 (t, $^{3}J_{(H1, H2)/(H2, H3)}$ = 8 Hz, 1H, H_2), 7.49 (d, $^{3}J_{(H9, H11)/(H10, H12)}$ = 8 Hz, 2H, $H_{9,}$ H_{10}), 6.88 (s, 2H, H_{15}, H_{16}), 5.72 (d, ^{3}J = 6 Hz, 1H, $H_{2'}$), 5.63 (d, ^{3}J = 6 Hz, 1H, $H_{3'}$), 5.58 (d, ^{3}J = 6 Hz, 1H, $H_{5'}$),

5.42 (d, ^{3}J = 6 Hz, $H_{6'}$), 2.79 (m, 1H, $H_{8'}$), 2.23 (s, 3H, $H_{7'}$), 1.22 (d, ^{3}J = 7 Hz, 3H, $H_{9'}$), 1.14 (d, ^{3}J = 7 Hz, 3H, $H_{10'}$); $^{13}C\{^{1}H\}$ NMR ($CDCl_3$, 100.6 MHz): δ (ppm) = 169.3 (C_{14}, C_{17}), 157.3 (C_1), 152.8 (C_5), 139.8 (C_3), 134.4 (C_{15}, C_{16}), 131.9 (C_{13}), 130.7 (C_8), 128.8 (C_2), 127.1 (C_4), 126.5 (C_9, C_{10}), 125.7 (C_{11}, C_{12}), 106.3 ($C_{4'}$), 103.0 ($C_{1'}$), 87.7, 87.1 ($C_{2'}$, $C_{6'}$), 84.6, 83.9 ($C_{3'}$, $C_{5'}$), 31.0 ($C_{8'}$), 22.7, 21.9 ($C_{9'}$, $C_{10'}$), 18.8 ($C_{7'}$); MS (ESI^+): *m/z* 544.0634 $[M– 2Cl – H]^+$ (m_{ex} = 544.0674); elemental analysis calculated for $C_{26}H_{25}Cl_2N_3O_2RuS·1.5H_2O$: C 48.60, H 4.39, N 6.54, S 4.99%; Found: C 48.70, H 4.29, N 6.55, S 4.98%.

Bromido[N-(4-(maleimidyl)phenyl)pyridine-2-carbothioamide](η^6-p-cymene)ruthenium(II) bromide, ***2b***

The synthesis was performed according to the general procedure using *N*-(4-(maleimidyl)phenyl)pyridine-2-carbothioamide (111 mg, 0.36 mmol) and $[Ru(\eta^6\text{-}p\text{-cymene})Br_2]_2$ dimer (142 mg, 0.18 mmol) to afford **2b** as a red-orange powder.

Yield: 238 mg (91%); m. p.: 179-182 °C (decomp.); ^{1}H NMR ($CDCl_3$, 400.13 MHz): δ (ppm) = 9.57 (d, $^{3}J_{(H3, H4)}$ = 8 Hz, 1H, H_4), 9.50 (d, $^{3}J_{(H1, H2)}$ = 6 Hz, 1H, H_1), 8.08 (t, $^{3}J_{(H2, H3)/(H3, H4)}$ = 8 Hz, 1H, H_3), 8.00 (d, $^{3}J_{(H9, H11)/(H10, H12)}$ = 8 Hz, 2H, H_{11}, H_{12}), 7.61 (t, $^{3}J_{(H1, H2)/(H2, H3)}$ = 6 Hz, 1H, H_2), 7.50 (d, $^{3}J_{(H9, H11)/(H10, H12)}$ = 8 Hz, 2H, $H_{9,}$ H_{10}), 6.89 (s, 2H, H_{15}, H_{16}), 5.78 (d, ^{3}J = 6 Hz, 1H, $H_{2'}$), 5.67 (m, 2H, $H_{3'}$, $H_{5'}$), 5.52 (d, ^{3}J = 6 Hz, 1H, $H_{6'}$), 2.84 (m, 1H, $H_{8'}$), 2.27 (s, 3H, H7'), 1.22 (d, ^{3}J = 7 Hz, 3H, $H_{9'}$), 1.16 (d, ^{3}J = 7 Hz, 3H, $H_{10'}$); $^{13}C\{^{1}H\}$ NMR ($CDCl_3$, 100.6 MHz): δ (ppm) = 169.1 (C_{14}, C_{17}), 158.5 (C_1), 153.5 (C_5), 139.8 (C_3), 136.5 (C_{13}), 134.4 (C_{15}, C_{16}), 131.4 (C_8), 129.2 (C_2), 127.5 (C_4), 126.5 (C_9, C_{10}), 126.4 (C_{11}, C_{12}), 107.3 ($C_{4'}$), 103.0 ($C_{1'}$), 87.8, 87.2 ($C_{2'}$, $C_{6'}$), 85.0, 84.9 ($C_{3'}$, $C_{5'}$), 31.3 ($C_{8'}$), 22.8, 22.0 ($C_{9'}$, $C_{10'}$); MS (ESI^+): *m/z* 544.0633 $[M – 2Br – H]^+$ (m_{ex} = 544.0638); elemental analysis calculated for $C_{26}H_{25}Br_2N_3O_2RuS·1.1H_2O$: C 43.12, H 3.79, N 5.80, S 4.43%; Found: C 43.17, H 3.74, N 5.80, S 4.52%.

Iodido[N-(4-(maleimidyl)phenyl)pyridine-2-carbothioamide](η^6-p-cymene)ruthenium(II) iodide, ***2c***

The synthesis was performed according to the general procedure using *N*-(4-(maleimidyl)phenyl)pyridine-2-carbothioamide (93 mg, 0.30 mmol) and $[Ru(\eta^6\text{-}p\text{-cymene})I_2]_2$ dimer (147 mg, 0.15 mmol) to afford **2c** as a red powder.

Yield: 192 mg (77%); m. p.: 191–194 °C (decomp.); ^{1}H NMR ($CDCl_3$, 400.13 MHz): δ (ppm) = 9.51 (d, $^{3}J_{(H3, H4)}$ = 8 Hz, 1H, H_4), 9.50 (d, $^{3}J_{(H1, H2)}$ = 6 Hz, 1H, H_1), 8.07 (t, $^{3}J_{(H2, H3)/(H3, H4)}$ = 8 Hz, 1H, H_3), 8.01 (d, $^{3}J_{(H9, H11)/(H10, H12)}$ = 9 Hz, 2H, H_{11}, H_{12}), 7.61 (t, $^{3}J_{(H1, H2)/(H2, H3)}$ = 6 Hz, 1H, H_2), 7.53 (d, $^{3}J_{(H9, H11)/(H10, H12)}$ = 9 Hz, 2H, $H_{9,}$ H_{10}), 6.89 (s, 2H, H_{15}, H_{16}), 5.82 (d, ^{3}J = 6 Hz, 1H, $H_{2'}$), 5.70 (m, 2H, $H_{3'}$/$H_{5'}$), 5.61 (d ^{3}J = 6 Hz, 1H, $H_{6'}$), 2.94 (m, 1H, $H_{8'}$), 2.35 (s, 3H, H7'), 1.24 (d, ^{3}J = 7 Hz, 3H, $H_{9'}$), 1.19 (d, ^{3}J = 7 Hz, 3H, $H_{10'}$); ^{13}C{^{1}H} NMR ($CDCl_3$, 100.6 MHz): δ (ppm) = 190.4 (C_6), 169.2 (C_{14}, C_{17}), 159.5 (C_1), 153.5 (C_5), 139.4 (C_3), 134.4 (C_{15}, C_{16}), 131.3 (C_{13}), 139.0 (C_8), 127.6 (C_2), 126.6 (C_4), 126.5 (C_9, C_{10}), 126.1 (C_{11}, C_{12}), 108.2 ($C_{4'}$), 103.1 ($C_{1'}$), 87.5, 87.4 ($C_{2'}$, $C_{6'}$), 85.9, 85.4 ($C_{3'}$, $C_{5'}$), 31.7 ($C_{8'}$), 23.0, 22.2 ($C_{9'}$, $C_{10'}$), 19.9 ($C_{7'}$); MS (ESI$^+$): *m/z* 544.0633 $[M – 2I – H]^+$ (m_{ex} = 544.0639); elemental analysis calculated for $C_{26}H_{25}I_2N_3O_2RuS·1.5H_2O$: C 37.83, H 3.42, N 5.09, S 3.88%; Found: C 37.83, H 3.09, N 5.06, S 3.76%.

Chlorido[N-(4-(maleimidyl)phenyl)pyridine-2-carbothioamide](η^6-p-cymene)osmium(II) chloride, ***2d***

The synthesis was performed according to the general procedure using *N*-(4-(maleimidyl)phenyl)pyridine-2-carbothioamide (93 mg, 0.30 mmol) and [Os(η^6-*p*-cymene)Cl_2]$_2$ dimer (119 mg, 0.15 mmol) to afford **2d** as a dark violet powder.

Yield: 160 mg (74%); m. p.: 206–210 °C (decomp.); ^{1}H NMR ($CDCl_3$, 400.13 MHz): δ (ppm) = 9.73 (brs, 1H, H_4), 9.22 (d, $^{3}J_{(H1, H2)}$ = 5 Hz, 1H, H_1), 8.11 (t, $^{3}J_{(H2, H3)/(H3, H4)}$ = 8 Hz, 1H, H_3), 8.00 (d, $^{3}J_{(H9, H11)/(H10, H12)}$ = 8 Hz, 2H, H_{11}, H_{12}), 7.54 (t, $^{3}J_{(H1, H2)/(H2, H3)}$ = 6 Hz, 1H, H_2), 7.50 (d, $^{3}J_{(H9, H11)/(H10, H12)}$ = 8 Hz, 2H, $H_{9,}$ H_{10}), 6.87 (s, 2H, H_{15}, H_{16}), 5.87 (d, ^{3}J = 6 Hz, 1H, $H_{2'}$), 5.77 (d, ^{3}J = 6 Hz; 1H, $H_{3'}$), 5.72 (d, ^{3}J = 6 Hz, 1H, $H_{5'}$), 5.57 (d, ^{3}J = 6 Hz, 1H, $H_{6'}$), 2.70 (m, 1H, $H_{8'}$), 2.29 (s, 3H, H7'), 1.22 (d, ^{3}J = 7 Hz, 3H, $H_{9'}$), 1.13 (d, ^{3}J = 7 Hz, 3H, $H_{10'}$); ^{13}C{^{1}H} NMR ($CDCl_3$, 100.6 MHz): δ (ppm) = 169.2 (C_{14}, C_{17}), 158.5 (C_1), 153.8 (C_5), 134.0 (C_3), 134.4 (C_{15}, C_{16}), 130.8 (C_{13}), 139.8 (C_8), 127.5 (C_2), 126.6 (C_4), 126.5 (C_9, C_{10}), 125.9 (C_{11}, C_{12}), 108.5 ($C_{4'}$), 96.0 ($C_{1'}$), 79.7, 78.6 ($C_{2'}$, $C_{6'}$), 76.4, 74.3 ($C_{3'}$, $C_{5'}$), 31.1 ($C_{8'}$), 23.1, 22.1 ($C_{9'}$, $C_{10'}$), 18.8($C_{7'}$); MS (ESI$^+$): *m/z* 634.1197 $[M – 2Cl – H]^+$ (m_{ex} = 634.1203); elemental analysis calculated for $C_{26}H_{25}Cl_2N_3O_2OsS·0.75H_2O$: C 43.48, H 3.72, N 5.85, S 4.46%; Found: C 43.50, H 3.91, N 5.70, S 4.31%.

Iodido[N-(4-(maleimidyl)phenyl)pyridine-2-carbothioamide](η^6-p-cymene)osmium(II) iodide, ***2e***

The synthesis was performed according to the general procedure using *N*-(4-(maleimidyl)phenyl)pyridine-2-carbothioamide (62 mg, 0.20 mmol) and [Os(η^6-*p*-cymene)I_2]$_2$ dimer (116 mg, 0.10 mmol) to afford **2e** as a deep violet powder.

Yield: 145 mg (80%); m. p.: 203–207 °C (decomp.); ^{1}H NMR ($CDCl_3$, 400.13 MHz): δ (ppm) = 9.65 (d, $^3J_{(H3, H4)}$ = 8 Hz, 1H, H_4), 9.33 (dd, $^3J_{(H1, H2)}$ = 7.0 Hz, $^4J_{(H1, H3)}$ = 1 Hz, 1H, H_1), 8.08 (t, $^3J_{(H2, H3)/(H3, H4)}$ = 8 Hz, 1H, H_3), 8.05 (d, $^3J_{(H9, H11)/(H10, H12)}$ = 9 Hz, 2H, H_{11}, H_{12}), 7.55 (t, $^3J_{(H1, H2)/(H2, H3)}$ = 8 Hz, 1H, H_2), 7.55 (d, $^3J_{(H9, H11)/(H10, H12)}$ = 9 Hz, 2H, H_9, H_{10}), 6.90 (s, 2H, H_{15}, H_{16}), 5.93 (d, ^3J = 6 Hz, 1H, $H_{2'}$), 5.82 (d, ^3J = 6 Hz, 1H, $H_{3'}$), 5.78 (d, ^3J = 6 Hz, 1H, $H_{5'}$), 5.71 (d, ^3J = 6 Hz, 1H, $H_{6'}$), 2.85 (m, 1H, $H_{8'}$), 2.42 (s, 3H, $H_{7'}$), 1.25 (d, ^3J = 7 Hz, 3H, $H_{9'}$), 1.20 (d, ^3J = 7 Hz, 3H, $H_{10'}$); ^{13}C{^{1}H} NMR ($CDCl_3$, 100.6 MHz): δ (ppm) = 169.2 (C_{14}, C_{17}), 160.1 (C_1), 153.7 (C_5), 139.4 (C_3), 134.4 (C_{15}, C_{16}), 131.1 (C_{13}), 129.8 (C_8), 127.8 (C_9, C_{10}), 126.3 (C_{11}, C_{12}), 99.4 ($C_{4'}$), 95.2 ($C_{1'}$), 79.7, 79.2 ($C_{2'}$, $C_{6'}$), 77.3, 77.1 ($C_{3'}$, $C_{5'}$), 31.6 ($C_{8'}$), 23.1, 22.2 ($C_{9'}$, $C_{10'}$), 19.7 ($C_{7'}$); MS (ESI$^+$): *m/z* 634.1197 [M – 2I – H]$^+$ (m_{ex} = 634.1171); elemental analysis calculated for $C_{26}H_{25}I_2N_3O_2OsS{\cdot}H_2O$: C 34.48, H 3.00, N 4.64, S 3.54%; Found: C 34.31, H 2.88, N 4.55, S 3.61%.

Chlorido[N-(4-(maleimidyl)phenyl)pyridine-2-carbothioamide](η^6-biphenyl)ruthenium(II) chloride, ***2f***

The synthesis was performed according to the general procedure using *N*-(4-(maleimidyl)phenyl)pyridine-2-carbothioamide (93 mg, 0.30 mmol) and [Ru(η^6-biphenyl)Cl_2]$_2$ dimer (98 mg, 0.15 mmol) to afford **2f** as a red-brown powder.

Yield: 90 mg (45%); m. p.: 178–183 °C (decomp.); ^{1}H NMR (MeOH-d_4, 400.13 MHz): δ (ppm) = 9.49 (d, $^3J_{(H3, H4)}$ = 8 Hz, 1H, H_4), 8.41 (d, $^3J_{(H1, H2)}$ = 9 Hz, 1H, H_1), 8.30 (td, $^3J_{(H2, H3)/(H3, H4)}$ = 8 Hz, $^4J_{(H1, H3)}$ = 1 Hz, 1H, H_3), 7.72-7.67(m, 5H, H_2, $H_{8'}$, $H_{12'}$, H_9, H_{10}), 7.61-7.59 (m, 2H, H_{11}, H_{12}), 7.50-7.45 (m, 3H, $H_{9'}$, $H_{10'}$, $H_{11'}$), 7.03 (s, 2H, H_{15}, H_{16}), 6.51 (d, ^3J = 6 Hz, 1H, $H_{3'}$/$H_{5'}$), 6.44 (d, ^3J = 6 Hz, 1H, $H_{3'}$/$H_{5'}$), 6.31(t, ^3J = 6 Hz, 1H, $H_{2'}$/ $H_{6'}$), 6.27 (t, ^3J = 6 Hz, 1H, $H_{2'}$/ $H_{6'}$), 6.17 (t, ^3J = 6 Hz, 1H, $H_{1'}$); ^{13}C {^{1}H} NMR (MeOH-d_4, 100.6 MHz): δ (ppm) = 193.5 (C_6), 170.9 (C_{14}, C_{17}), 160.0 (C_4), 155.1 (C_1), 153.4 (C_5), 141.1 (C_3), 135.7 (C_{15}, C_{16}), 125.0 (C_2), 90.9, 89.7 ($C_{2'}$, $C_{6'}$), 88.3 ($C_{1'}$), 86.7, 86.1 ($C_{3'}$, $C_{5'}$); MS (ESI$^+$): *m/z* 564.0321 [M – 2Cl – H]$^+$ (m_{ex} = 564.0301);

elemental analysis calculated for $C_{28}H_{21}Cl_2N_3O_2RuS \cdot 1.3H_2O$: C 51.04, H 3.61, N 6.38, S 4.87%; Found: C 50.73, H 3.44, N 6.58, S 5.05%.

Chlorido[N-(4-(maleimidyl)phenyl)pyridine-2-carbothioamide](η^6-biphenyl)osmium(II) chloride, ***2g***

The synthesis was performed according to the general procedure using *N*-(4-(maleimidyl)phenyl)pyridine-2-carbothioamide (93 mg, 0.30 mmol) and [Os(η^6-biphenyl)Cl_2]$_2$ dimer (111 mg, 0.15 mmol) to afford **2g** as a dark violet powder.

Yield: 84 mg (38%); m. p.: 197–200 °C (decomp.); ^{1}H NMR (MeOH-d_4, 400.13 MHz): δ (ppm) = 9.27 (dd, $^3J_{(H3, H4)}$ = 6 Hz, $^4J_{(H2, H4)}$ = 1Hz, 1H, H_4), 8.38 (dd, $^3J_{(H1, H2)}$ = 8 Hz, $^4J_{(H1, H3)}$ = 1 Hz, 1H, H_1), 8.13 (td, $^3J_{(H2, H3)/(H3, H4)}$ = 7 Hz, 1H, H_3), 7.60-7.51 (m, 5H, H_2, $H_{8'}$, $H_{12'}$, H_9, H_{10}), 7.50-7.46 (m, 2H, H_{11}, H_{12}), 7.35-7.32 (m, 3H, $H_{9'}$, $H_{10'}$, $H_{11'}$), 6.93 (s, 2H, H_{15}, H_{16}), 6.60(d, ^3J = 5 Hz, 1H, $H_{3'}$/$H_{5'}$), 6.54 (d, ^3J = 5 Hz, 1H, $H_{3'}$/$H_{5'}$), 6.33-6.28 (m, 2H, $H_{2'}$, $H_{6'}$), 6.20 (t, $^3J_{(H1', H2')/(H1', H6')}$ = 6 Hz, 1H, $H_{1'}$); ^{13}C {^{1}H} NMR (MeOH-d_4, 100.6 MHz): δ (ppm) = 171.0 (C_{14}, C_{17}), 160.7 (C_4), 141.3 (C_3), 135.8 (C_{15}, C_{16}), 125.4 (C_2), 82.0, 81.1 ($C_{2'}$, $C_{6'}$), 80.4 ($C_{1'}$), 79.3, 78.7 ($C_{3'}$, $C_{5'}$); MS (ESI$^+$): *m/z* 654.0884 [M – 2Cl – H]$^+$ (m_{ex} = 654.0899); elemental analysis calculated for $C_{28}H_{21}Cl_2N_3O_2OsS \cdot H_2O$: C 45.28, H 3.12, N 5.66, S 4.32%; Found: C 45.12, H 3.18, N 5.57, S 4.40%.

Stability in aqueous solution

Stability experiments in aqueous solutions were carried out by dissolving **2a**, **2d** and **2f** (1–2 mg/mL) in DMSO-d_6/D_2O (5/95) and ^{1}H NMR spectra were recorded over a period of up to 96 h.

Amino acid binding studies

For Cys reactivity studies, solutions of **2a**, **2b, 2d** and **2f** (1 mg/mL) in DMSO-d_6/D_2O (5/95) were treated with 1.2 equivalents of Cys and ^{1}H NMR spectra were recorded for up to 2 h. The reaction of **2a** with L-histidine and L-methionine was studied under the same conditions for up to 96 h by ^{1}H NMR spectroscopy. For ESI-MS binding studies between **2a** and L-histidine and L-methionine, the samples were incubated at room temperature in water at molar ratios of 1 : 1 (100 μM). Before analysis, the samples were diluted 9 : 1 with 30% methanol/H_2O.

Sulforhodamine B Cytotoxicity Assay

HCT116 and MDA MB 231 cells were supplied by ATCC and Dr. Adam Patterson, University of Manchester, UK, respectively, and were grown in αMEM (Life Technologies) supplemented with 5% fetal calf serum (Moregate Biotech). Cells were seeded at 750 (HCT116) or 10000 (MDA MB 231) cells/well in 96-well plates and left to settle for 24 h at 37 °C and 5% CO_2. Compounds were added to the plates in a series of 3-fold dilutions in 0.5% DMSO or less for 72 h before the assay was terminated by addition of 10% trichloroacetic acid (Merck Millipore) at 4 °C for 1 h. Cells were stained with 0.4% sulforhodamine B (Sigma-Aldrich) in 1% acetic acid for 30 min in the dark at room temperature, then washed in 1% acetic acid to remove unbound dye. The stain was solubilized in unbuffered Tris base (10 mM; Serva) for 30 min. on a plate shaker in the dark and quantitated on a BioTek EL808 microplate reader at an absorbance of 490 nm with a reference wavelength of 450 nm. The 10-point IC_{50} values were calculated by fitting the inhibition data relative to no inhibitor controls and proliferation at the time of compound addition to a four-parameter logistic sigmoidal dose-response curve using Prism 6.03 (GraphPad).

Hen egg white lysozyme binding studies

Hen egg white lysozyme (HEWL) was crystallized by hanging-drop vapor diffusion using a reservoir solution containing 0.8 M NaCl, 0.1 M sodium acetate pH 4.7 mixed with an equal volume of HEWL (100 mg/ml) [46]. Crystals formed within 24 h and were then transferred into the reservoir solution containing **2a** (1.2 mg, 1.0 mg/mL). After a period of 24 h the crystals began to turn yellow and then darkened over a period of 5 days after which they were transferred into a cryoprotectant of 0.8 M NaCl, 0.1 M sodium acetate at pH 4.7 and 20% glycerol prior to flash-freezing in liquid nitrogen. X-ray diffraction data was collected on the microcrystallography beamline MX2 and processed using MOSFLM [47]. Image integration was performed using MOSFLM [48], followed by structure determination with molecular replacement using a the model 4NHI as a search model in PHASER [49]. This model was refined by successive rounds of refinement and model building in REFMAC5 [50] and COOT [51]. An anomalous difference map was generated using FFT to identify the location of the Ru moiety [52], which was refined at an occupancy of 0.5 resulting in a b-factor of 28.6 $Å^2$. The coordinates have been deposited in the Protein Data Bank (PDB) under the accession code 5KJ9.

For ESI-MS binding studies, HEWL (50 µM) and **2a** (1 : 2) were incubated at 37 °C for 5 days in 18.2 MΩ water. Before analysis with a Bruker micrOTOF-Q II mass spectrometer in positive ESI mode, the samples were diluted 1:10 with water. Samples were analyzed after 2, 6, 24 h and 5 days. The Data Analysis 4.0 software package from Bruker Daltonics (Bremen, Germany) was used for processing of the data sets. Maximum entropy deconvolution was applied with automatic data point spacing and 10000 instrument resolving power.

References

[1] F. Arnesano, G. Natile, Coord. Chem. Rev. 253 (2009) 2070-2081.

[2] R. Trondl, P. Heffeter, C.R. Kowol, M.A. Jakupec, W. Berger, B.K. Keppler, Chem. Sci. 5 (2014) 2925-2932.

[3] C.G. Hartinger, N. Metzler-Nolte, P.J. Dyson, Organometallics 31 (2012) 5677-5685.

[4] M. Hanif, M.V. Babak, C.G. Hartinger, Drug Discovery Today 19 (2014) 1640-1648.

[5] A.A. Nazarov, C.G. Hartinger, P.J. Dyson, J. Organomet. Chem. 751 (2014) 251-260.

[6] A.F. Peacock, P.J. Sadler, Chem. Asian J. 3 (2008) 1890-1899.

[7] A. Weiss, R.H. Berndsen, M. Dubois, C. Müller, R. Schibli, A.W. Griffioen, P.J. Dyson, P. Nowak-Sliwinska, Chem. Sci. 5 (2014) 4742-4748.

[8] A. Weiss, X. Ding, J.R. Beijnum, I. Wong, T.J. Wong, R.H. Berndsen, O. Dormond, M. Dallinga, L. Shen, R.O. Schlingemann, R. Pili, C.-M. Ho, P.J. Dyson, H. Bergh, A.W. Griffioen, P. Nowak-Sliwinska, Angiogenesis 18 (2015) 233-244.

[9] C.S. Allardyce, P.J. Dyson, Dalton Trans. 45 (2016) 3201-3209.

[10] Z. Adhireksan, G.E. Davey, P. Campomanes, M. Groessl, C.M. Clavel, H. Yu, A.A. Nazarov, C.H. Yeo, W.H. Ang, P. Droge, U. Rothlisberger, P.J. Dyson, C.A. Davey, Nat. Commun. 5 (2014) 3462.

[11] C.G. Hartinger, P.J. Dyson, Chem. Soc. Rev. 38 (2009) 391-401.

[12] S. van Zutphen, J. Reedijk, Coord. Chem. Rev. 249 (2005) 2845-2853.

[13] H. Maeda in, Drug Delivery in Oncology, Wiley-VCH Verlag GmbH & Co. KGaA, 2011, pp. 65-84.

[14] L. Fang, M. Jing, X. Bengang, Curr. Pharm. Des. 21 (2015) 1866-1888.

[15] A. Ito, M. Shinkai, H. Honda, T. Kobayashi, J. Biosci. Bioeng. 100 (2005) 1-11.

[16] C. Corot, P. Robert, J.-M. Idée, M. Port, Adv. Drug Delivery Rev. 58 (2006) 1471-1504.

[17] D.J. Thorek, A. Chen, J. Czupryna, A. Tsourkas, Ann. Biomed. Eng. 34 (2006) 23-38.

[18] J. Xie, J. Huang, X. Li, S. Sun, X. Chen, Curr. Med. Chem. 16 (2009) 1278-1294.

[19] S. Sharifi, H. Seyednejad, S. Laurent, F. Atyabi, A.A. Saei, M. Mahmoudi, Contrast Media Mol. Imaging 10 (2015) 329-355.

[20] C.S. Allardyce, P.J. Dyson, D.J. Ellis, S.L. Heath, Chem. Commun. (2001) 1396-1397.

[21] D. Peer, J.M. Karp, S. Hong, O.C. Farokhzad, R. Margalit, R. Langer, Nat. Nanotechnol. 2 (2007) 751-760.

[22] T.M. Allen, Nat. Rev. Cancer 2 (2002) 750-763.

[23] F. Kratz, J. Control. Release 132 (2008) 171-183.

[24] A.K. Bytzek, G. Koellensperger, B.K. Keppler, C.G. Hartinger, Journal of Inorganic Biochemistry (2016) doi:10.1016/j.jinorgbio.2016.1002.1037.

[25] M. Groessl, C.G. Hartinger, K. Polec-Pawlak, M. Jarosz, B.K. Keppler, Electrophoresis 29 (2008) 2224-2232.

[26] J.D. Holding, W.E. Lindup, C. van Laer, G.C. Vreeburg, V. Schilling, J.A. Wilson, P.M. Stell, Br. J. Clin. Pharmacol. 33 (1992) 75-81.

[27] F. Kratz, Expert Opin. Therap. Pat. 12 (2002) 433-439.

[28] W.H. Ang, E. Daldini, L. Juillerat-Jeanneret, P.J. Dyson, Inorg. Chem. 46 (2007) 9048-9050.

[29] A. Warnecke, I. Fichtner, D. Garmann, U. Jaehde, F. Kratz, Bioconjug. Chem. 15 (2004) 1349-1359.

[30] D. Garmann, A. Warnecke, G.V. Kalayda, F. Kratz, U. Jaehde, J. Control. Release 131 (2008) 100-106.

[31] R. Graeser, N. Esser, H. Unger, I. Fichtner, A. Zhu, C. Unger, F. Kratz, Invest. New Drugs 28 (2010) 14-19.

[32] F. Kratz, I. Fichtner, A. Zhu, A. Craig, Mol. Cancer Ther. 6 (2007) 3421s-3421s.

[33] M. Hanif, A.A. Nazarov, A. Legin, M. Groessl, V.B. Arion, M.A. Jakupec, Y.O. Tsybin, P.J. Dyson, B.K. Keppler, C.G. Hartinger, Chem. Commun. 48 (2012) 1475-1477.

[34] C. Scolaro, A. Bergamo, L. Brescacin, R. Delfino, M. Cocchietto, G. Laurenczy, T.J. Geldbach, G. Sava, P.J. Dyson, J. Med. Chem. 48 (2005) 4161-4171.

[35] C. Scolaro, T.J. Geldbach, S. Rochat, A. Dorcier, C. Gossens, A. Bergamo, M. Cocchietto, I. Tavernelli, G. Sava, U. Rothlisberger, P.J. Dyson, Organometallics 25 (2005) 756-765.

[36] S. Moon, M. Hanif, M. Kubanik, H. Holtkamp, T. Soehnel, S.M.F. Jamieson, C.G. Hartinger, ChemPlusChem 80 (2015) 231-236.

[37] S.M. Meier, M. Hanif, Z. Adhireksan, V. Pichler, M. Novak, E. Jirkovsky, M.A. Jakupec, V.B. Arion, C.A. Davey, B.K. Keppler, C.G. Hartinger, Chem. Sci. 4 (2013) 1837-1846.

[38] M.A. Bennett, A.K. Smith, J. Chem. Soc., Dalton Trans. (1974) 233-241.

[39] M.G. Mendoza-Ferri, C.G. Hartinger, A.A. Nazarov, R.E. Eichinger, M.A. Jakupec, K. Severin, B.K. Keppler, Organometallics 28 (2009) 6260-6265.

[40] Y. Fu, A. Habtemariam, A.M.B.H. Basri, D. Braddick, G.J. Clarkson, P.J. Sadler, Dalton Trans. 40 (2011) 10553-10562.

[41] I. Romero-Canelon, L. Salassa, P.J. Sadler, J. Med. Chem. 56 (2013) 1291-1300.

[42] M.H. Klingele, S. Brooker, Eur. J. Org. Chem. (2004) 3422-3434.

[43] SAINT, Area detector integration software, Siemens Analytical Instruments Inc., Madison, WI, USA, 1995,

[44] G.M. Sheldrick, SADABS, Program for semi-empirical absorption correction, University of Göttingen, Göttingen, Germany, 1997,

[45] G.M. Sheldrick, Acta Crystallogr., Sect. A: Found. Crystallogr. A64 (2008) 112-122.

[46] E. Arnold, D.M. Himmel, D.G. Rossmann (Eds.), Volume F: Crystallography of Biological Macromolecules, 2012.

[47] A.G.W. Leslie, H.R. Powell, Evolving Methods for Macromolecular Crystallography, Dordrecht: Springer, 2007, pp. 192.

[48] T.G.G. Battye, L. Kontogiannis, O. Johnson, H.R. Powell, A.G.W. Leslie, Acta Crystallogr., Sect. D: Biol. Crystallogr. 67 (2011) 271-281.

[49] A.J. McCoy, R.W. Grosse-Kunstleve, P.D. Adams, M.D. Winn, L.C. Storoni, R.J. Read, J. Appl. Crystallogr. 40 (2007) 658-674.

[50] G.N. Murshudov, A.A. Vagin, E.J. Dodson, Acta Crystallogr., Sect. D: Biol. Crystallogr. 53 (1997) 240-255.

[51] P. Emsley, K. Cowtan, Acta Crystallogr., Sect. D: Biol. Crystallogr. 60 (2004) 2126-2132.

[52] R.J. Read, A.J. Schierbeek, J. Appl. Crystallogr. 21 (1988) 490-495.